Supporting Information

Biocompatibility and photo-induced antibacterial activity of lignin-stabilized noble metal nanoparticles

Diamela Rocca[a,b], Julie P. Vanegas[†a,c], Kelsey Fournier[†a], M. Cecilia Becerra[b], Juan C. Scaiano[a] and Anabel E. Lanterna*[a]

Table of Content

Synthesis and characterization of MNP@lignin

In order to select the best conditions for the synthesis of MNP@lignin, different methods were screened for the thermal- and photo-synthesis of nanocomposites utilizing alkali lignin. Table S1 summarized different conditions studied.

Table S1. Synthesis conditions screened for MNP@Alkali composites.

(Metal precursor/lignin)[a]	Irradiation conditions	T (ºC)	t (min)
10, 5, 1, 0.1	Dark	55-60	10
10, 5, 2, 1, 0.5, 0.2, 0.1	400	25	20
10, 5, 2, 1, 0.5, 0.2, 0.1	465	28	20
5, 1, 0.5, 0.1	530	28	20
10, 5, 2, 1, 0.5, 0.2, 0.1	730	25	20

[a] mg of precursor salt ($AgNO_3$ or $HAuCl_4$) per mg of lignin, for a total amount of 0.1 mg lignin per mL.

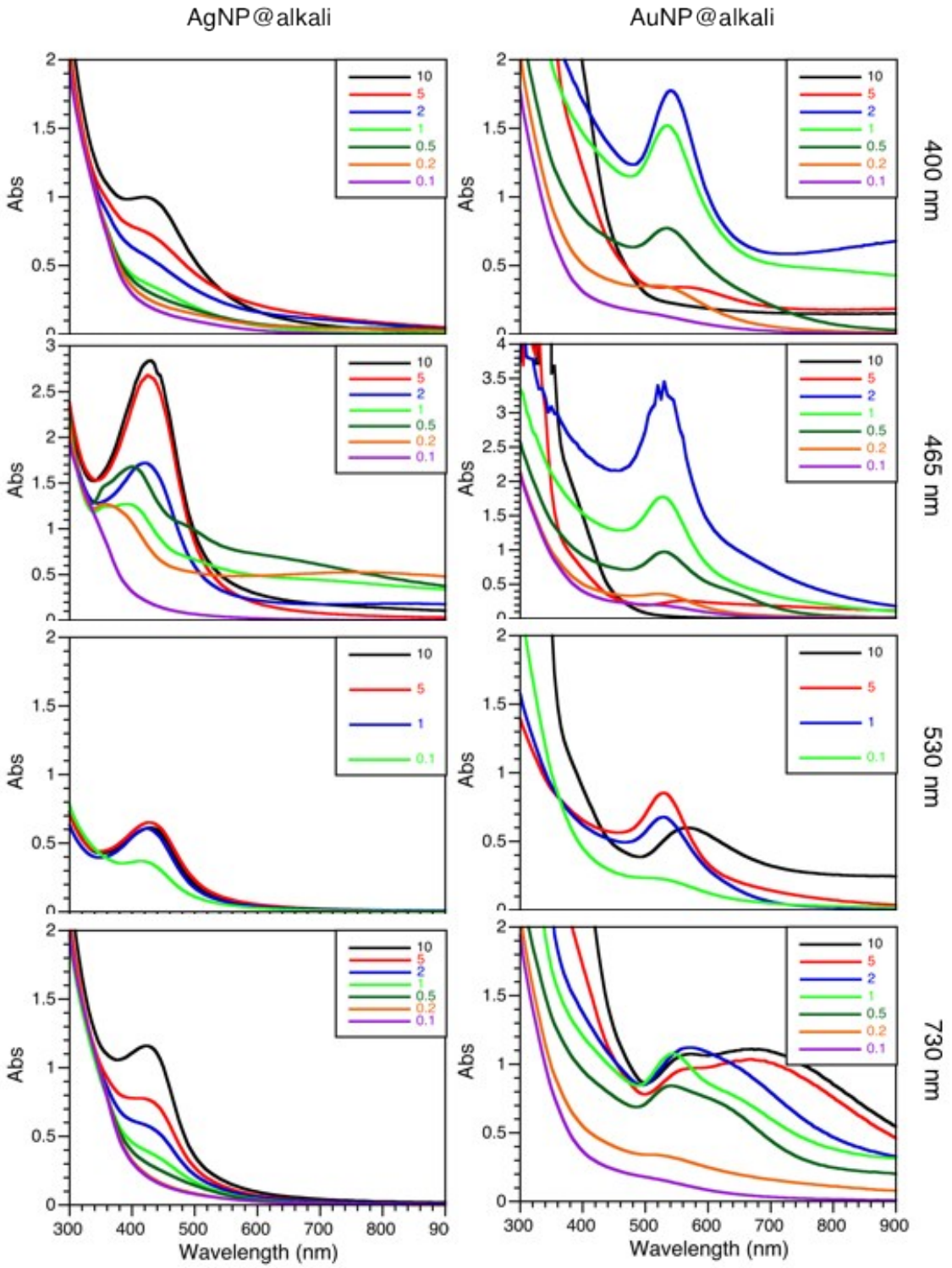

Figure S 1. UV-Vis absorption spectra of MNP@alkali solutions obtained by irradiation with different wavelengths.

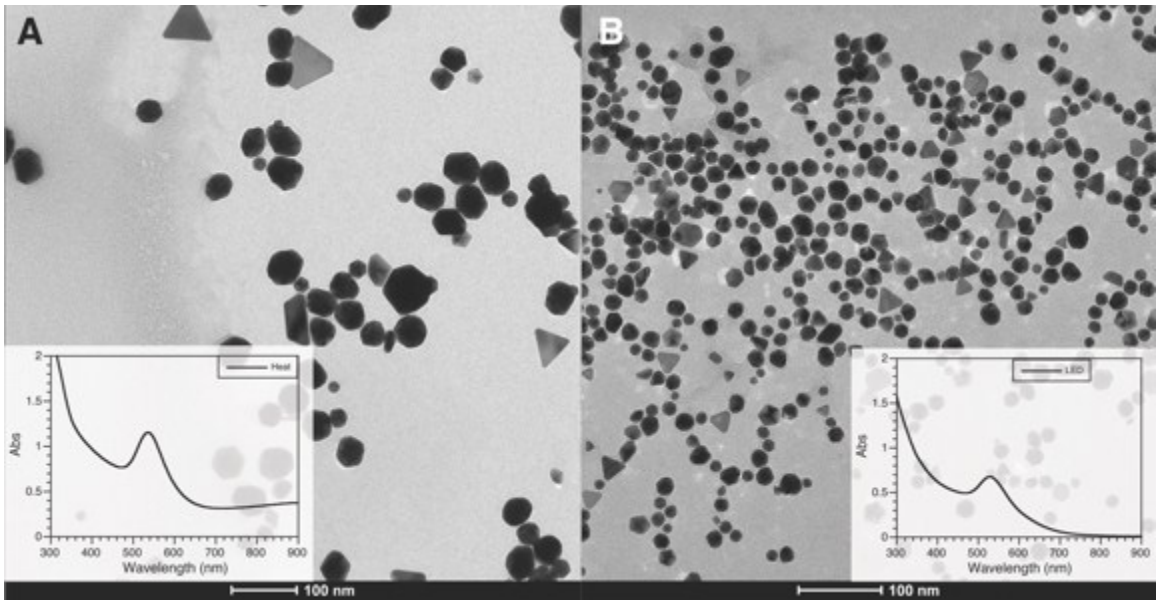

Figure S 2. TEM images of the AuNP@Alkali synthesized following protocols described in table S1: A) thermal reaction, $HAuCl_4$/lignin = 1; B) photochemical reaction, $HAuCl_4$/lignin = 0.5(530 nm irradiation). Scale bar: 100 nm.

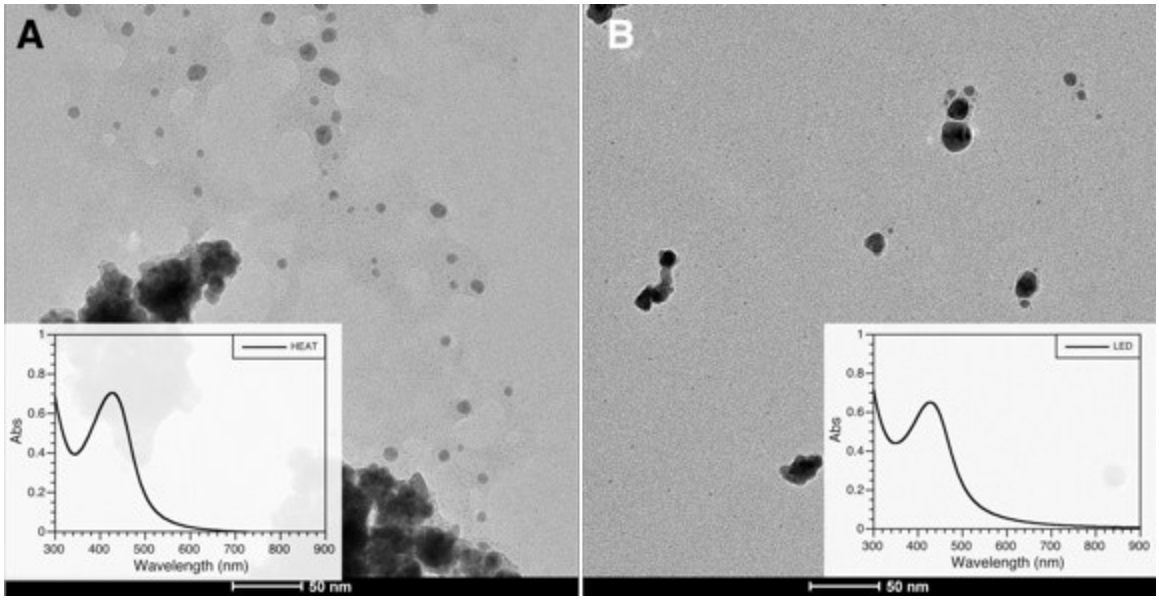

Figure S 3. TEM images of the AgNP@Alkali synthesized following protocols described in table S1: A) thermal reaction, $AgNO_3$/lignin = 10 B) photochemical reaction, $AgNO_3$/lignin = 5 (465 nm irradiation). Scale bar: 50 nm.

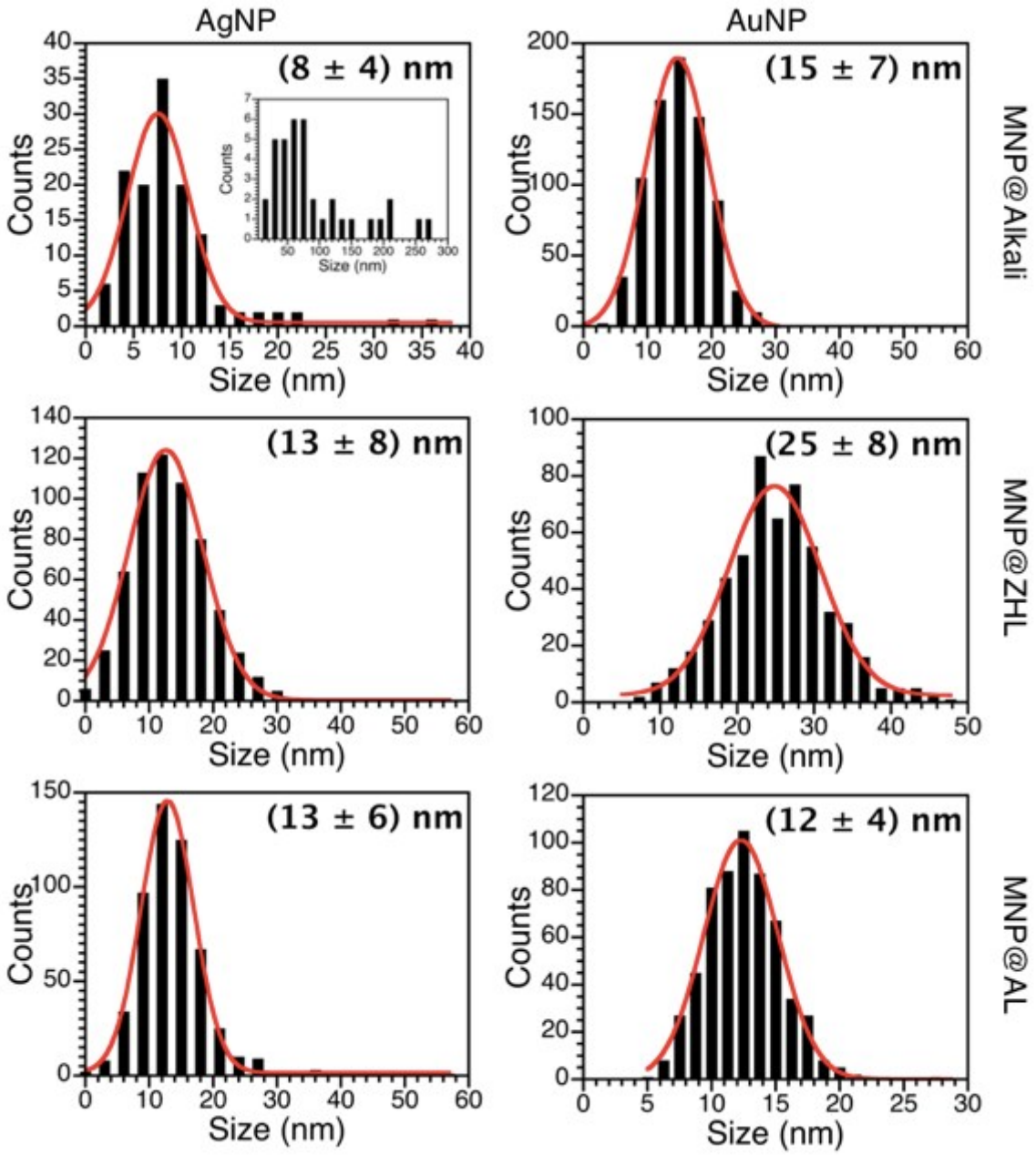

Figure S 4. Particle size distribution for the MNP@lignin nanocomposites determined by measuring 200-400 nanoparticles from different TEM images.

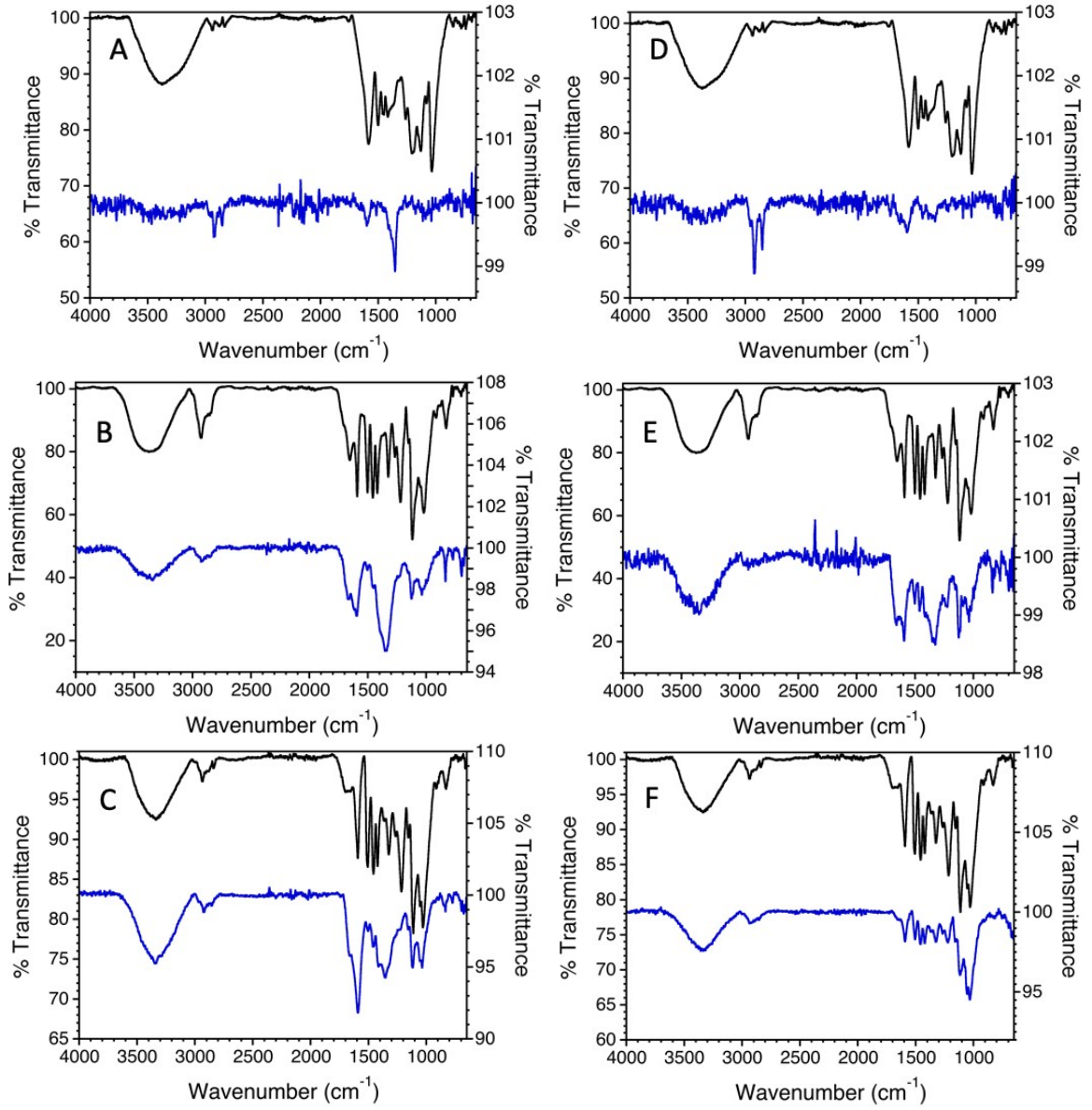

Figure S 5. ATR FT-IR spectra of the lignin alone (black) and the MNP@lignin composites (blue). (A) AgNP@alkali, (B) AgNP@AL, (C) AgNP@ZHL, (D) AuNP@alkali, (E) AuNP@AL and (F) AuNP@ZHL.

Calculation of the NP concentration

The particle concentration was calculated based on the following assumptions: i) the MNP are perfectly spherical and ii) the size distribution is monodisperse. Based on the previously reported methodology[1] we used equation 1 to determine the number of atoms per NP:

$$N = \left(\frac{R_{NP}}{r_A}\right)^3 \qquad (1)$$

where R_{NP} is the NP radius (average radius determined by TEM imaging) and r_A is the covalent atomic radius of the metal (0.144 nm for Au and 0.153 nm for Ag). The NP concentration can be estimated by equation 2:

$$C_{NP} = \frac{N_{NP}}{N_A} = \frac{N_{atoms}}{NxN_A} = \frac{moles\ Au^{3+}\ (or\ Ag^{+})\ x\ N_A}{l} x \frac{1}{NxN_A} \qquad (2)$$

The total amount of Au or Ag was determined by ICP.

Stability of MNP@lignin composites in different biological media

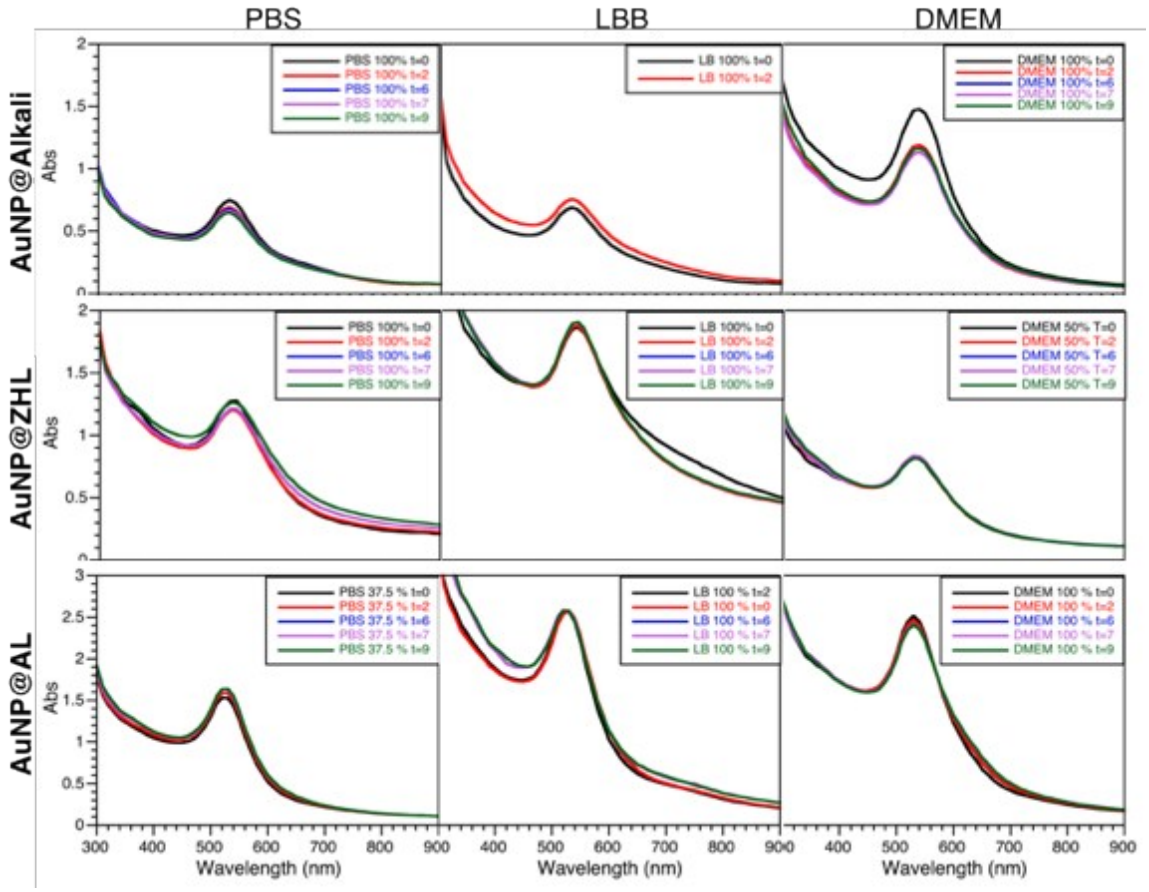

Figure S 6. Time evolution of UV-Vis spectra of different AuNP@lignin dispersed in different biological media.

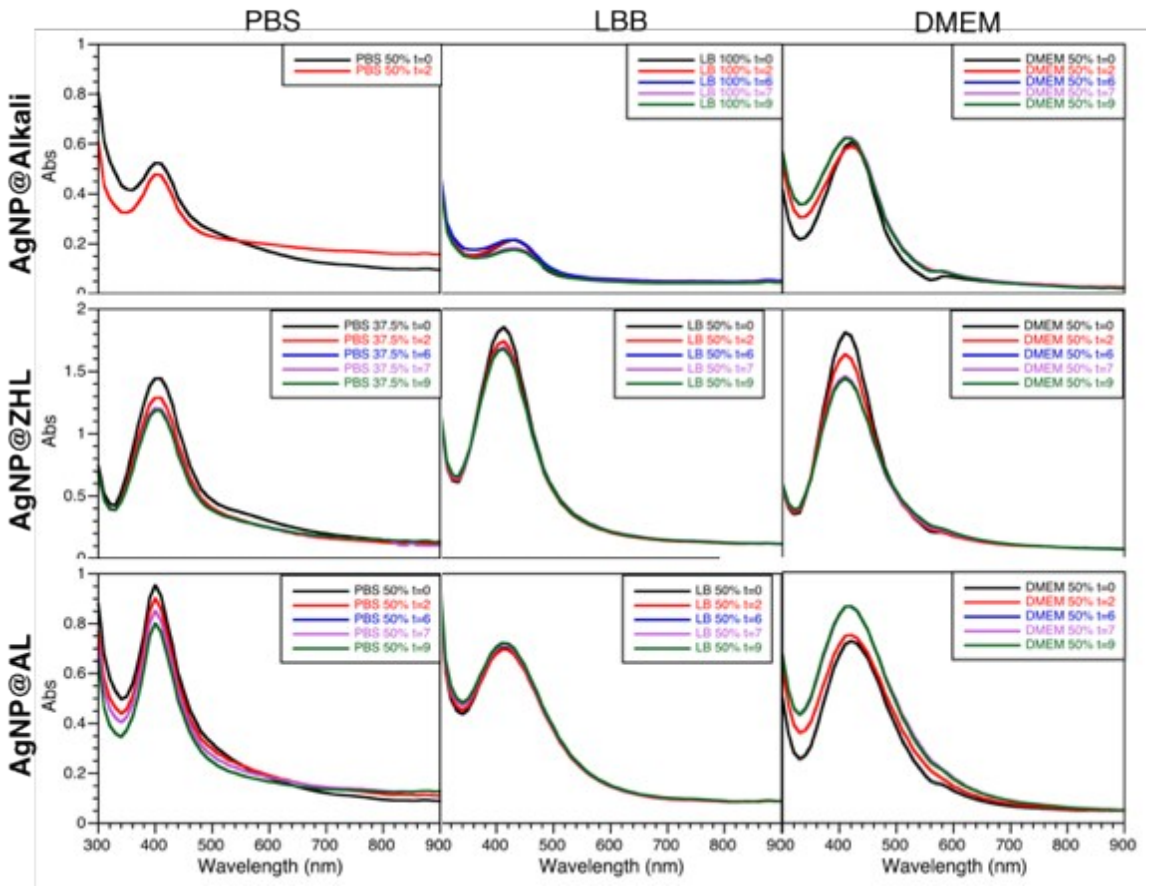

Figure S 7. Time evolution of UV-Vis spectra of different AgNP@lignin dispersed in different biological media.

Antimicrobial activity

Table S2. Different concentrations used to determine the antimicrobial activity of MNP@lignin composites expressed in µg of metal per mL and in nM of MNP.

MNP@lignin	[a]A (µg/mL)	B (µg/mL)	A (nM)	B (nM)	Lignin loading (wt%)[b]
AuNP@Alkali	223	22	8.0	0.8	53
AuNP@ZHL	337	34	2.6	0.26	16
AuNP@AL	499	50	35.0	3.5	23
AgNP@Alkali	0.2	0.1	0.03[c]	0.02[d]	98
AgNP@ZHL	19	9	9.8	4.9	88
AgNP@AL	24	12	2.9[c]	1.5[d]	98[e]

[a] Determined by ICP-OES measurements. [b] Values obtained assuming spherical volume of the core MNP (diameter calculated from TEM imaging) and shell (hydrodynamic volume calculated from DLS). [c]MIC [d]SubMIC. Based on amount of Ag. Reported MIC for $HAuCl_4$ is around 0.2 µg/mL.[2] Tested MIC for $AgNO_3$ is 4.1 µg/mL (based on silver content). [e] Bottom wt% silver content considering particle aggregation can reduce this number.

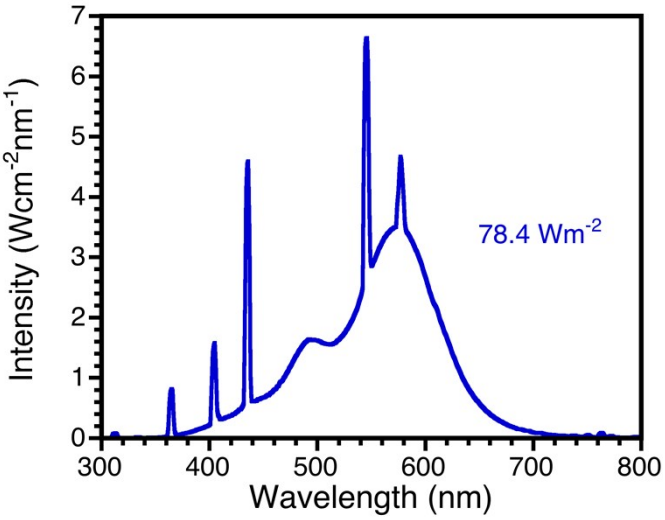

Figure S 8. Emission spectrum of the white light lamps used for illumination. Total irradiance ~ 78 Wm^{-2}.

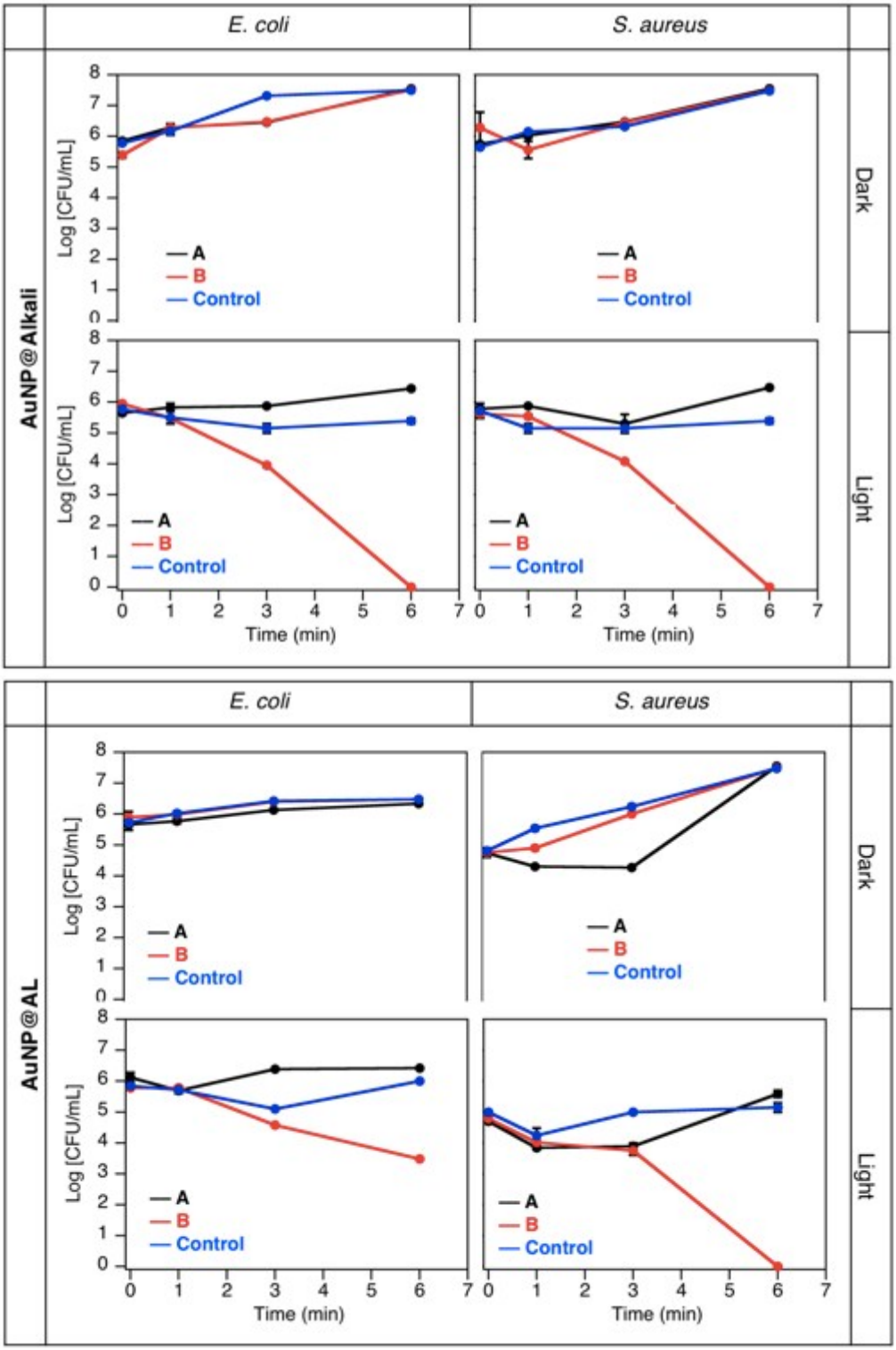

Figure S 9. Bacteria time-kill profiles for *E. coli* and *S. aureus* up to 6 h in the presence of AuNP@alkali and AuNP@AL at A and B concentrations given in table S3.

ROS production

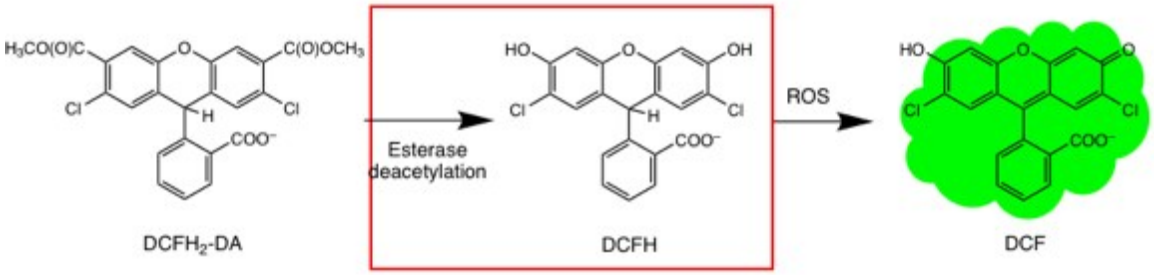

Figure S 10. 2,7-dichlorodihydrofluorescein diacetate ($DCFH_2$-DA) undergoes deacetylation, in the presence of bacteria esterase (red box). Consecutive oxidation with ROS generate a highly fluorescent molecule (DCF).

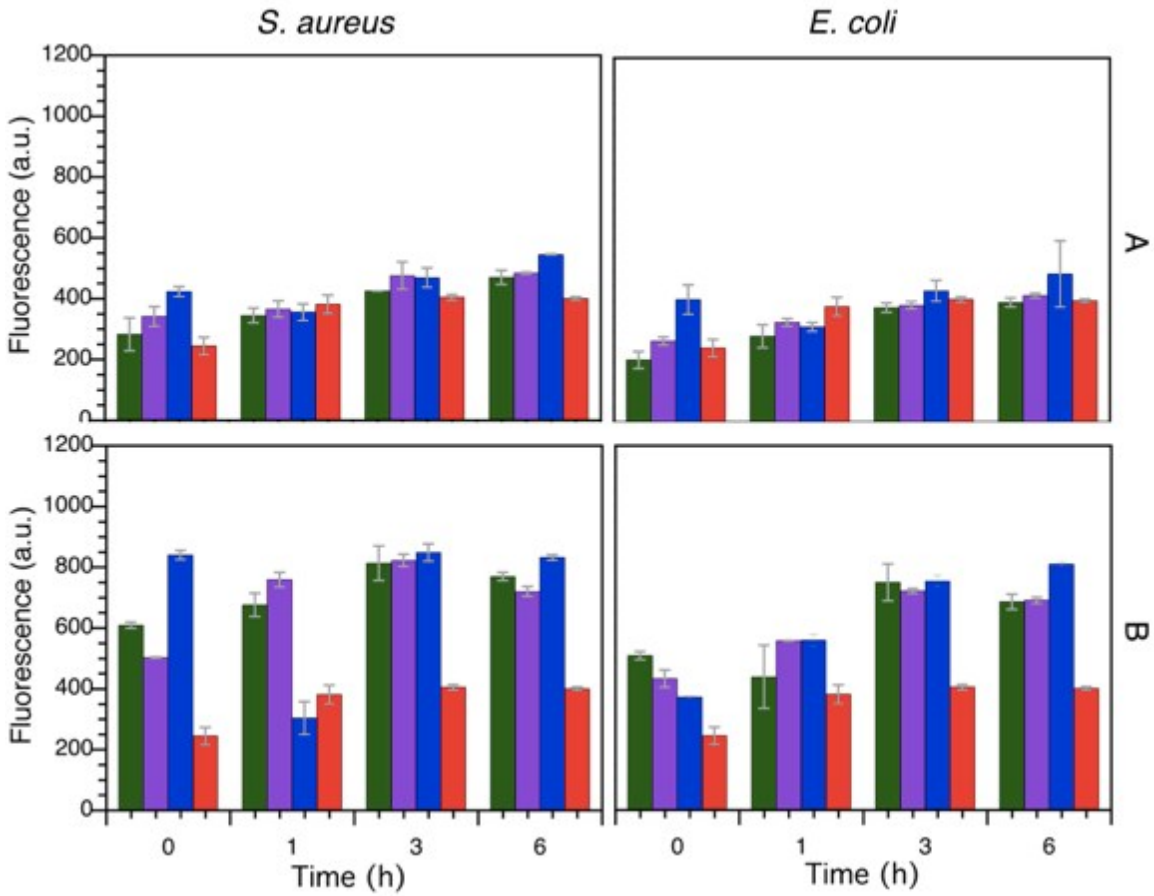

Figure S 11. ROS production for samples of *S. aureus* and *E. coli* phototreated with white light in the presence of AuNP@alkali (green), AuNP@AL (purple), AuNP@ZHL (blue), and in the absence of particles (red) at concentrations A and B given in table S3.

Cell viability

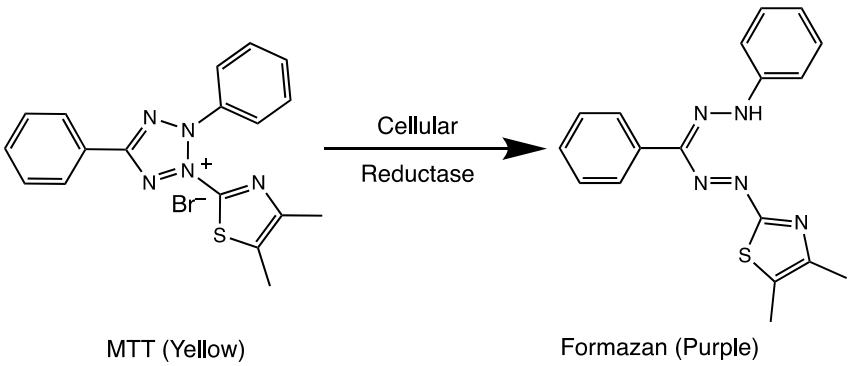

Figure S 12. MTT assay based on the reduction of tetrazolium salt to formazan (absorbance at 570 nm) in living cells.

REFERENCES

1. Pacioni, N. L.; Gonzalez-Bejar, M.; Alarcon, E.; McGilvray, K. L.; Scaiano, J. C., Surface Plasmons Control the Dynamics of Excited Triplet States in the Presence of Gold Nanoparticles *J. Am. Chem. Soc.* **2010,** 132, 6298.

2. Shareena Dasari, T. P.; Zhang, Y.; Yu, H., Antibacterial Activity and Cytotoxicity of Gold (I) and (III) Ions and Gold Nanoparticles *Biochem. Pharmacol.* **2015,** 4.